Vol. 8 (2015) *Acta Physica Polonica B Proceedings Supplement* No 4

PROBING BFKL DYNAMICS AT HADRONIC COLLIDERS*

Christophe Royon

Kansas University, Lawrence, USA
and
Institute of Physics, Academy of Science, Prague, Czech Republic
and
The H. Niewodniczański Institute of Nuclear Physics PAN, Kraków, Poland

(Received November 12, 2015)

After recalling briefly the BFKL fits to the HERA forward jet data, we describe different possibilities to probe the BFKL dynamics at hadronic colliders, namely Mueller–Navelet jet, and jet–gap–jet events. We also discuss briefly the jet veto measurement as performed by the ATLAS Collaboration at the LHC.

DOI:10.5506/APhysPolBSupp.8.1001
PACS numbers: 12.38.–t, 13.85.–t, 12.38.Qk

1. Forward jets at HERA

In this section, we recall briefly the previous results that we obtained concerning forward jets at HERA [1–4].

Forward jets at HERA are an ideal observable to look for BFKL resummation effects. The interval in rapidity between the scattered lepton and the jet in the forward region is large, and when the photon virtuality Q^2 is close to the transverse jet momentum k_{T}, the DGLAP cross section is small because of the k_{T} ordering of the emitted gluons. In this short report, we will only discuss the phenomenological aspects and all detailed calculations can be found in Ref. [2–4] for forward jets at HERA.

The BFKL NLL [1] longitudinal transverse cross section reads

$$\frac{d\sigma^{\gamma * p\to JX}_{\mathrm{T,L}}}{dx_J dk_{\mathrm{T}}^2} \sim \frac{f_{\mathrm{eff}}}{k_{\mathrm{T}}^2 Q^2}\int d\gamma \left(\frac{Q^2}{k_{\mathrm{T}}^2}\right)^{\gamma} \phi^{\gamma}_{\mathrm{T,L}}(\gamma)\; e^{\bar{\alpha}(k_{\mathrm{T}}Q)\chi_{\mathrm{eff}}[\gamma,\bar{\alpha}(k_{\mathrm{T}}Q)]Y}\,, \qquad (1)$$

* Presented at EDS Blois 2015: The 16$^{\mathrm{th}}$ Conference on Elastic and Diffractive Scattering, Borgo, Corsica, France, June 29–July 4, 2015.

where x_J is the proton momentum fraction carried by the forward jet, $\chi_{\rm eff}$ is the effective BFKL NLL kernel and the ϕs are the transverse and longitudinal impact factors taken at LL. The effective kernel $\chi_{\rm eff}(\gamma, \bar{\alpha})$ is defined from the NLL kernel $\chi_{\rm NLL}(\gamma, \omega)$ by solving the implicit equation numerically

$$\chi_{\rm eff}(\gamma, \bar{\alpha}) = \chi_{\rm NLL}\left[\gamma, \bar{\alpha}\ \chi_{\rm eff}(\gamma, \bar{\alpha})\right] . \tag{2}$$

The integration over γ in Eq. (1) is performed numerically. It is possible to fit directly $d\sigma/dx$ measured by the H1 Collaboration using this formalism with one single parameter, the normalisation. The values of $\chi_{\rm NLL}$ are taken at NLL [1] using different resummation schemes to remove spurious singularities defined as S3 and S4 [5]. Contrary to LL BFKL, it is worth noticing that the coupling constant $\alpha_{\rm s}$ is taken using the renormalisation group equations, the only free parameter in the fit being the normalisation.

The NLL fits [2–4] can nicely describe the H1 data [3] for the S4 and S3 schemes [2–4] ($\chi^2 = 0.48/5$ and $\chi^2 = 1.15/5$ respectively per degree of freedom with statistical and systematic errors added in quadrature). The curve using an LL fit is indistinguishable in Fig. 1 from the result of the BFKL NLL fit. The DGLAP NLO calculation fails to describe the H1 data at lowest x (see Fig. 1). We also checked the effect of changing the scale in the exponential of Eq. (1) from $k_{\rm T}Q$ to $2k_{\rm T}Q$ or $k_{\rm T}Q/2$ which leads to a difference of 20% on the cross section, while changing the scale to

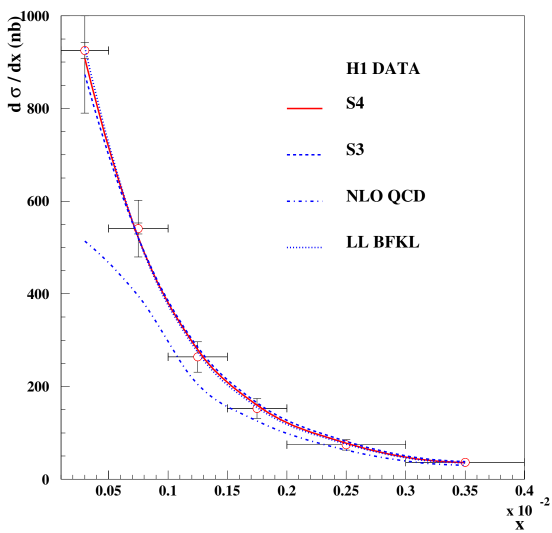

Fig. 1. Comparison between the H1 $d\sigma/dx$ measurement with predictions for BFKL LL, BFKL NLL (S3 and S4 schemes) and DGLAP NLO calculations (see the text). S4, S3 and LL BFKL cannot be distinguished in that figure.

k_T^2 or Q^2 modifies the result by less than 5% which is due to the cut on $0.5 < k_T^2/Q^2 < 5$. Implementing the higher-order corrections in the impact factor due to exact gluon dynamics in the $\gamma^* \to q\bar{q}$ transition [6] changes the result by less than 3%.

The H1 Collaboration also measured the forward jet triple differential cross section [3] and the results are given in Fig. 2. We keep the same normalisation coming from the fit to $d\sigma/dx$ to predict the triple differential cross section. The BFKL LL formalism leads to a good description of the data when $r = k_T^2/Q^2$ is close to 1 and deviates from the data when r is

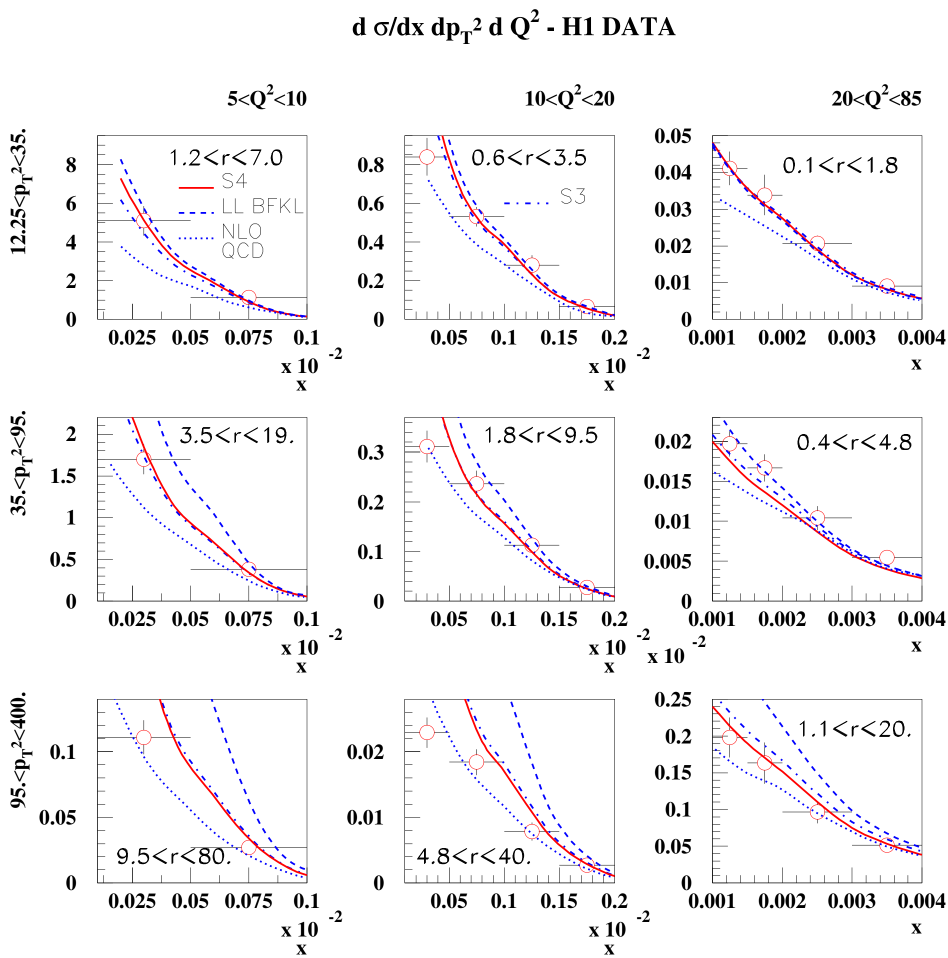

Fig. 2. Comparison between the H1 measurement of the triple differential cross section with predictions for BFKL LL, BFKL NLL and DGLAP NLO calculations (see the text).

further away from 1. This effect is expected since DGLAP radiation effects are supposed to occur when the ratio between the jet k_{T} and the virtual photon Q^2 are further away from 1. The BFKL NLL calculation including the Q^2 evolution via the renormalisation group equation leads to a good description of the H1 data on the full range. We note that the higher order corrections are small when $r \sim 1$, when the BFKL effects are supposed to dominate. By contrast, they are significant as expected when r is different from one, *i.e.* when DGLAP evolution becomes relevant. We notice that the DGLAP NLO calculation fails to describe the data when $r \sim 1$, or in the region where BFKL resummation effects are expected to appear.

In addition, we checked the dependence of our results on the scale taken in the exponential of Eq. (1). The effect is a change of the cross section of about 20% at low p_{T} increasing to 70% at highest p_{T}. Taking the correct gluon kinematics in the impact factor leads, as expected, to a better description of the data at high p_{T} [2–4].

2. Mueller–Navelet jets at Tevatron and LHC

Mueller–Navelet jets are another ideal processes to study BFKL resummation effects [4]. Two jets with a large interval in rapidity and with similar transverse momenta are considered. A typical observable to look for BFKL effects is the measurement of the azimuthal correlations between both jets. The DGLAP prediction is that this distribution should peak towards π — *i.e.* jets are back-to-back — whereas multi-gluon emission via the BFKL mechanism leads to a smoother distribution. The azimuthal correlation is an ideal variable to look for BFKL resummation effects since it is less sensitive to experimental uncertainties such as the jet energy scale as an example [4]. The effect of the energy conservation in the BFKL equation [4] is large when R goes away from 1. The effect is to reduce the effective value of $\Delta\eta$ between the jets and thus the decorrelation effect. However, it is worth noticing that this effect is negligible when the ratio of the jet p_{T}s is close to 1. It is thus important to perform this measurement as a function of the ratio of the jet p_{T}.

3. Jet veto measurements in ATLAS

The ATLAS Collaboration measured the so-called jet veto cross section [7], namely the events with two high p_{T} jets, well separated in rapidity and with a veto on jet activity with p_{T} greater than a given threshold Q_0 between the two jets. The jet veto fraction is measured with respect to the standard dijet cross section, and it was advocated that it might be sensitive to BFKL dynamics. In Ref. [8], we computed the gluon emission at large angles (which are not considered in usual MC) using the Banfi–Marchesini–Smye equation, and we showed that the measurement can be effectively described by the gluon resummation and is thus not related to BFKL dynamics as shown in Fig. 3. The sensitivity to the BFKL resummation effects appears when one looks for gaps between jets or regions between central jets where little energy is deposited as described in the following section.

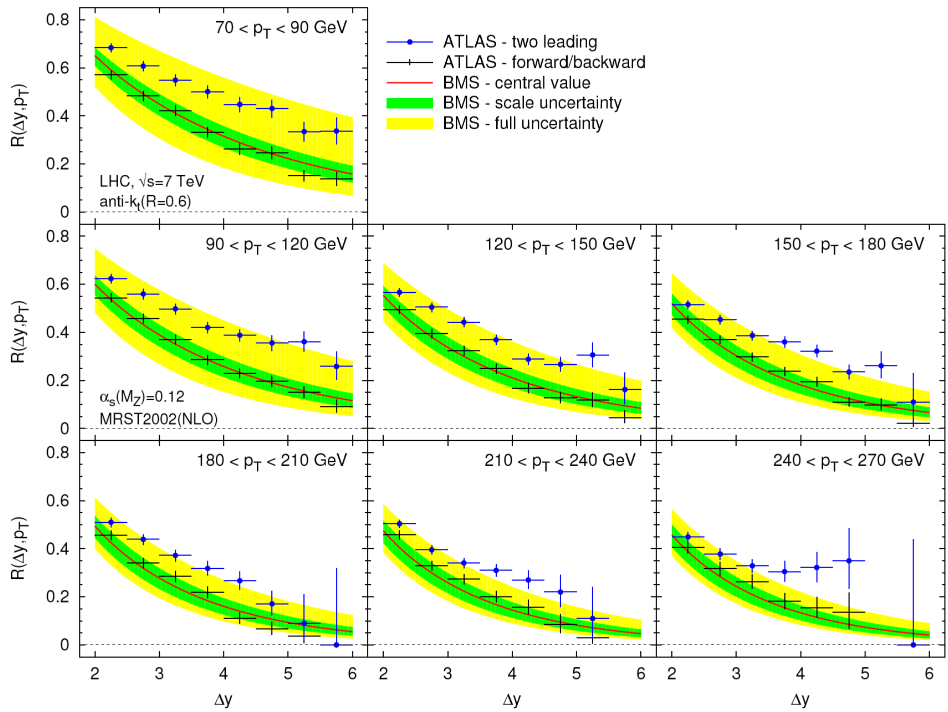

Fig. 3. (Colour on-line) Comparison of the resummed veto fraction with the ATLAS measurement, for a fixed veto energy of $E_{\mathrm{out}} = 20$ GeV, in different bins of p_{T}. The inner (green) uncertainty band is obtained taking into account only the renormalisation and factorization scale uncertainties, while the outer (yellow) band also includes the subleading logarithmic uncertainty. For the ATLAS data, circles represent the case where the two leading jets are selected while the one where the most forward and backward jets are selected are represented by crosses.

4. Jet–gap–jets at the Tevatron and the LHC

In this section, we describe a new possible measurement which can probe BFKL resummation effects and we compare our predictions with the existing D0 and CDF measurements [9].

4.1. BFKL NLL formalism

The production cross section of two jets with a gap in rapidity between them reads

$$\frac{d\sigma^{pp\to XJJY}}{dx_1 dx_2 dE_{\mathrm{T}}^2} = \mathcal{S} f_{\mathrm{eff}}\left(x_1, E_{\mathrm{T}}^2\right) f_{\mathrm{eff}}\left(x_2, E_{\mathrm{T}}^2\right) \frac{d\sigma^{gg\to gg}}{dE_{\mathrm{T}}^2}\,, \tag{3}$$

where $\sqrt{s}$ is the total energy of the collision, E_{T} the transverse momentum of the two jets, x_1 and x_2 their longitudinal fraction of momentum with respect to the incident hadrons, S the survival probability, and f the effective parton density functions [9]. The rapidity gap between the two jets is $\Delta\eta = \ln(x_1 x_2 s/p_{\mathrm{T}}^2)$.

The cross section is given by

$$\frac{d\sigma^{gg\to gg}}{dE_{\mathrm{T}}^2} = \frac{1}{16\pi}\left|A\left(\Delta\eta, E_{\mathrm{T}}^2\right)\right|^2 \tag{4}$$

in terms of the $gg \to gg$ scattering amplitude $A(\Delta\eta, p_{\mathrm{T}}^2)$.

In the following, we consider the high energy limit in which the rapidity gap $\Delta\eta$ is assumed to be very large. The BFKL framework allows to compute the $gg \to gg$ amplitude in this regime, and the result is known up to NLL accuracy

$$A = \frac{\alpha_{\mathrm{s}}^2}{E_{\mathrm{T}}^2} \sum_{p=-\infty}^{\infty} \int \frac{d\gamma}{2i\pi} \frac{\left[p^2 - (\gamma - 1/2)^2\right] \exp\left\{\bar{\alpha}\chi_{\mathrm{eff}}[2p]\Delta\eta\right\}}{\left[(\gamma - 1/2)^2 - (p - 1/2)^2\right]\left[(\gamma - 1/2)^2 - (p + 1/2)^2\right]} \tag{5}$$

with the complex integral running along the imaginary axis from $1/2 - i\infty$ to $1/2 + i\infty$, and with only even conformal spins contributing to the sum, and $\bar{\alpha} = \alpha_{\mathrm{s}} N_C/\pi$ the running coupling.

In this study, we performed a parametrised distribution of $d\sigma^{gg\to gg}/dE_{\mathrm{T}}^2$ so that it can be easily implemented in the Herwig Monte Carlo [10] since performing the integral over γ, in particular, would be too much time consuming in a Monte Carlo. The implementation of the BFKL cross section in a Monte Carlo is absolutely necessary to make a direct comparison with data. Namely, the measurements are sensitive to the jet size (for instance, experimentally the gap size is different from the rapidity interval between the jets which is not the case by definition in the analytic calculation).

4.2. Comparison with D0 and CDF measurements and predictions for the LHC

Let us first notice that the sum over all conformal spins is absolutely necessary. Considering only $p = 0$ in the sum of Eq. (5) leads to a wrong normalisation and a wrong jet E_{T} dependence, and the effect is more pronounced as $\Delta\eta$ diminishes.

The D0 Collaboration measured the jet–gap–jet cross section ratio with respect to the total dijet cross section, requesting for a gap between -1 and 1 in rapidity, as a function of the second leading jet E_{T}, and $\Delta\eta$ between the two leading jets for two different low and high E_{T} samples ($15 < E_{\mathrm{T}} < 20$ GeV and $E_{\mathrm{T}} > 30$ GeV). To compare with theory, we compute the following quantity

$$\mathrm{Ratio} = \frac{\textsf{BFKL NLL Herwig}}{\textsf{Dijet Herwig}} \times \frac{\mathrm{LO\ QCD}}{\mathrm{NLO\ QCD}} \tag{6}$$

in order to take into account the NLO corrections on the dijet cross sections, where BFKL NLL Herwig and Dijet Herwig denote the BFKL NLL and the dijet cross section implemented in Herwig [10]. The NLO QCD cross section was computed using the fNLOJet++ program [11].

The comparison with D0 data [9] is shown in Fig. 4. We find a good agreement between the data and the BFKL calculation. It is worth noticing that the BFKL NLL calculation leads to a better result than the BFKL LL one. The comparison with the CDF data [9] leads to similar conclusions.

Using the same formalism and assuming a survival probability of 0.03 at the LHC, it is possible to predict the jet–gap–jet cross section at the LHC. While both LL and NLL BFKL formalisms lead to a weak jet E_{T} or $\Delta\eta$

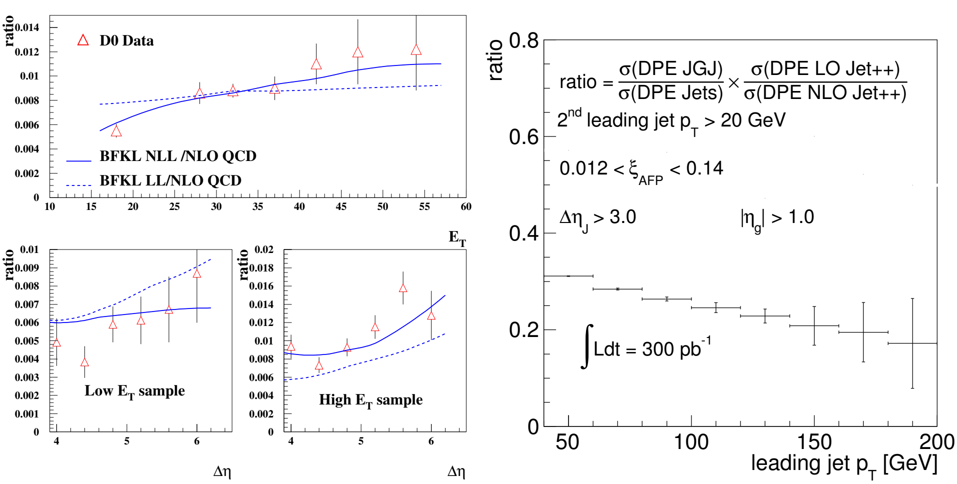

Fig. 4. Left: Comparisons between the D0 measurements of the jet–gap–jet event ratio with the NLL and LL BFKL calculations. The NLL calculation is in fair agreement with the data. The LL calculation leads to a worse description of the data. Right: Ratio of the jet–gap–jet to the inclusive jet cross sections at the LHC as a function of jet p_{T} in double Pomeron exchange events where the protons are detected in AFP.

dependence, the normalisation is found to be quite different leading to lower cross section for the BFKL NLL formalism. The ratio of the jet–gap–jet to the inclusive jet cross sections at the LHC as a function of jet p_{T} and $\Delta\eta$ is quite flat as shown in Ref. [9].

5. Jet–gap–jet event in diffractive processes

A new process of detecting jet–gap–jet events in diffractive double Pomeron exchange processes was introduced recently [12]. The idea is to tag the intact protons inside the CMS–TOTEM, CT-PPS or ATLAS (AFP) forward proton detectors [13] located at about 210 m from the ATLAS interaction point on both sides. The advantage of such processes is that they are quite clean since they are not "polluted" by proton remnants and it is possible to go to larger jet separation than for usual jet–gap–jet events. The normalisation for these processes comes from the fit to the D0 discussed in the previous section. The ratio between jet–gap–jet to inclusive jet events is shown in Fig. 3 requesting protons to be tagged in AFP for both samples. The ratio shows a weak dependence as a function of jet p_{T} (and also as a function of the difference in rapidity between the two jets). It is worth noticing that the ratio is about 20–30% showing that the jet–gap–jet events are much more present in the diffractive sample than in the inclusive one as expected. This measurement is part of the full diffractive program of the CMS–TOTEM, CT-PPS and AFP projects [14].

6. Conclusion

In this short article, we described many measurements that were performed at HERA, the Tevatron and the LHC to look for BFKL resummation effects such as the forward jet, the Mueller–Navelet or the jet–gap–jet cross section measurements. New possible observables were also proposed recently such as the measurement of the 3 jet cross section [15].

REFERENCES

[1] V.S. Fadin, L.N. Lipatov, *Phys. Lett. B* **429**, 127 (1998); M. Ciafaloni, *Phys. Lett. B* **429**, 363 (1998); M. Ciafaloni, G. Camici, *Phys. Lett. B* **430**, 349 (1998).

[2] O. Kepka, C. Marquet, R. Peschanski, C. Royon, *Phys. Lett. B* **655**, 236 (2007); *Eur. Phys. J. C* **55**, 259 (2008); A. Sabio Vera, F. Schwennsen, *Nucl. Phys. B* **776**, 170 (2007); *Phys. Rev. D* **77**, 014001 (2008); H. Navelet, R. Peschanski, C. Royon, S. Wallon, *Phys. Lett. B* **385**, 357 (1996); **366**, 329 (1996).

[3] A. Aktas *et al.* [H1 Collaboration], *Eur. Phys. J. C* **46**, 27 (2006).

[4] A.H. Mueller, H. Navelet, *Nucl. Phys. B* **282**, 727 (1987); C. Marquet, C. Royon, *Phys. Rev. D* **79**, 034028 (2009); B. Ducloué, L. Szymanowski, S. Wallon, *J. High Energy Phys.* **1305**, 096 (2013).

[5] G.P. Salam, *J. High Energy Phys.* **9807**, 019 (1998).

[6] C.D. White, R. Peschanski, R.S. Thorne, *Phys. Lett. B* **639**, 652 (2006).

[7] G. Aad *et al.*, *J. High Energy Phys.* **1109**, 053 (2011).

[8] Y. Hatta *et al.*, *Phys. Rev. D* **87**, 054016 (2013).

[9] O. Kepka, C. Marquet, C. Royon, *Phys. Rev. D* **83**, 034036 (2011); F. Chevallier, O. Kepka, C. Marquet, C. Royon, *Phys. Rev. D* **79**, 094019 (2009); B. Abbott *et al.*, *Phys. Lett. B* **440**, 189 (1998); F. Abe *et al.*, *Phys. Rev. Lett.* **80**, 1156 (1998).

[10] G. Marchesini *et al.*, *Comput. Phys. Commun.* **67**, 465 (1992).

[11] Z. Nagy, Z. Trocsanyi, *Phys. Rev. Lett.* **87**, 082001 (2001).

[12] C. Marquet, C. Royon, M. Trzebinski, R. Zlebcik, *Phys. Rev. D* **87**, 034010 (2013).

[13] ATLAS Coll., CERN-LHCC-2011-012; TOTEM Coll., CERN-LHCC-2014-020; CMS and TOTEM coll., CERN-LHCC-2014-021.

[14] For a review see the LHC Forward Physics Working Group report, preprint CERN-PH-LPCC-2015-001, SLAC-PUB-16364, DESY 15-167; S. Fichet *et al.*, *J. High Energy Phys.* **1502**, 165 (2015); *Phys. Rev. D* **89**, 114004 (2014); E. Chapon, O. Kepka, C. Royon, *Phys. Rev. D* **81**, 074003 (2010); O. Kepka, C. Royon, *Phys. Rev. D* **78**, 073005 (2008); C. Marquet, C. Royon, M. Saimpert, D. Werder, *Phys. Rev. D* **88**, 074029 (2013); A. Chuinard, C. Royon, R. Staszewski, `arXiv:1510.04218 [hep-ph]`.

[15] F. Caporale, G. Chachamis, B. Murdaca, A. Sabio Vera, `arXiv:1508.07711 [hep-ph]`.